Reactions of Aliphatic Thiyl Radicals in the Solid State: Photoisomerization of *trans*-4,5-Dihydroxy-1,2-dithiacyclohexane and Oxidation of Dithiothreitol

Lorena B. Barrón,[†] Kenneth C. Waterman,[‡] Thomas J. Offerdahl,[†] Eric Munson,[†] and Christian Schöneich*,[†]

Department of Pharmaceutical Chemistry, University of Kansas, 2095 Constant Avenue, Lawrence, Kansas 66047, and Pharmaceutical Research and Development, Pfizer, Incorporated, Eastern Point Road, Groton, Conneticut 06340

Received: April 18, 2005; In Final Form: July 21, 2005

A description of free-radical reactions in the solid state is important for some processes causing long-term stability problems of natural and synthetic products. Recent studies revealed that, in the solid state, mercaptooctadecanethiyl radicals, $C_{18}H_{37}S^{\bullet}$, do not abstract a hydrogen atom from mercaptooctadecane, $C_{18}H_{37}$-SH, but yield perthiyl radicals, $C_{18}H_{37}SS^{\bullet}$, via a net sulfur transfer (Faucitano et al. *ChemPhysChem* **2005**, *6*, 1100−1107). Here, we demonstrate that such a sulfur transfer is not a general phenomenon of thiyl-radical reactions in the solid state, providing experimental evidence for a solid-state hydrogen-transfer reaction between a dithiyl radical, generated through the photolysis of *trans*-4,5-dihydroxy-1,2-dithiacyclohexane (DTT_{ox}), and dithiothreitol. The photolysis of crystalline solid deposits of DTT_{ox} yields two isomers of 2,3-dihydroxy-1-mercaptotetrahydrothiophene with a combined quantum yield of $\Phi_F = 0.39 \pm 0.02$. This quantum yield was increased to $\Phi_F = 0.87 \pm 0.13$ when the solid deposits contained an additional dithiol, DL-1,4-dimercapto-2,3-butanediol (DTT), at a ratio of $DTT/DTT_{ox} = 10:1$. This increase in quantum yield depended, in part, on the presence of oxygen but was independent of residual moisture in the solid samples. Mechanistically, the formation of 2,3-dihydroxy-1-mercaptotetrahydrothiophene can be rationalized by the H transfer from DTT to a photochemically formed dithiyl radical from DTT_{ox}, yielding 2 equiv of monothiyl radicals from DTT, followed by a series of radical transformations.

Introduction

Free-radical reactions play an important role in the degradation or "aging" of synthetic and natural products. These processes may be triggered photochemically and/or through the (auto)oxidation of labile functional groups of the respective target molecules or impurities present in these materials. Much research effort has focused on the mechanisms and parameters controlling free-radical reactions in solution. However, a great deal of these reactions occur in nonfluid media such as polymers and even solids.[1,2] For example, many pharmaceutical drug candidates are formulated or preformulated in the solid state, where oxidative degradation is a well-known phenomenon. The fact that these formulations often contain multiple components, such as drug(s) and excipients, may render mechanistic investigations on such solid-state oxidation reactions quite complex compared with studies of single crystals.[3]

A fundamental reaction involved in many oxidation processes is the abstraction of a hydrogen atom.[1] Reactions performed in single crystals have provided important physicochemical details on the parameters controlling H-transfer reactions in the solid state. For example, intramolecular H-transfer processes triggered by the photolysis of ene-diones and related compounds show a strong dependency on the crystallographic distances between H acceptors and H donors, where the sum of the van der Waals radii of the reacting atoms may represent an upper limit for distances over which H-transfer reactions occur.[1] The resulting biradicals recombine to yield final products that have molecular dimensions similar to those of the reactants, which is consistent with the topochemical principle. The photolysis of undecanoyl peroxides provides an example for an intermolecular solid-state hydrogen transfer. Here, the selectivity of the intermolecular H transfer from a neighboring chain is the result of a rotational motion of the long-chain alkyl radicals to relieve local stress caused by the photochemical release of CO_2.[4]

To predict the solid-state reactivity of heterogeneous solid formulations, we need quantitative information on the generation and reactivity of specific pharmaceutically relevant reactive species in the solid state. Thiols represent a pharmaceutically and biologically highly abundant functional group that is easily oxidized to the respective thiyl radical through H transfer or combined electron/proton transfer.[5,6] This paper focuses on the solid-state reactivity of thiyl radicals. Recently, Faucitano et al. reported the quite unusual solid-state reaction between a thiyl radical ($RS^{\bullet}$) and a thiol (RSH), which did not proceed via hydrogen transfer but a net sulfur transfer to yield a perthiyl radical ($RSS^{\bullet}$).[7] This radical was identified by electron spin resonance spectroscopy on the basis of the analogy to a radical obtained during the γ irradiation of crystalline cystine dihydrochloride.[8] The net sulfur transfer was rationalized by a topochemical control of the reaction in the solid.[7] The present paper will show that such a sulfur transfer does not constitute a general pathway of solid-state thiyl-radical reactions. Instead, hydrogen transfer appears to be the predominant solid-state reaction between dithiyl radicals, photochemically generated from *trans*-4,5-dihydroxy-1,2-dithiacyclohexane (DTT_{ox}; species **1** in Scheme 1) and dithiothreitol (**6**).

* Corresponding author. Phone: (785) 864-4880. Fax: (785) 864-5736. E-mail: schoneic@ku.edu.
[†] University of Kansas.
[‡] Pfizer, Inc.

10.1021/jp052011q CCC: $30.25
Published on Web 09/24/2005

SCHEME 1

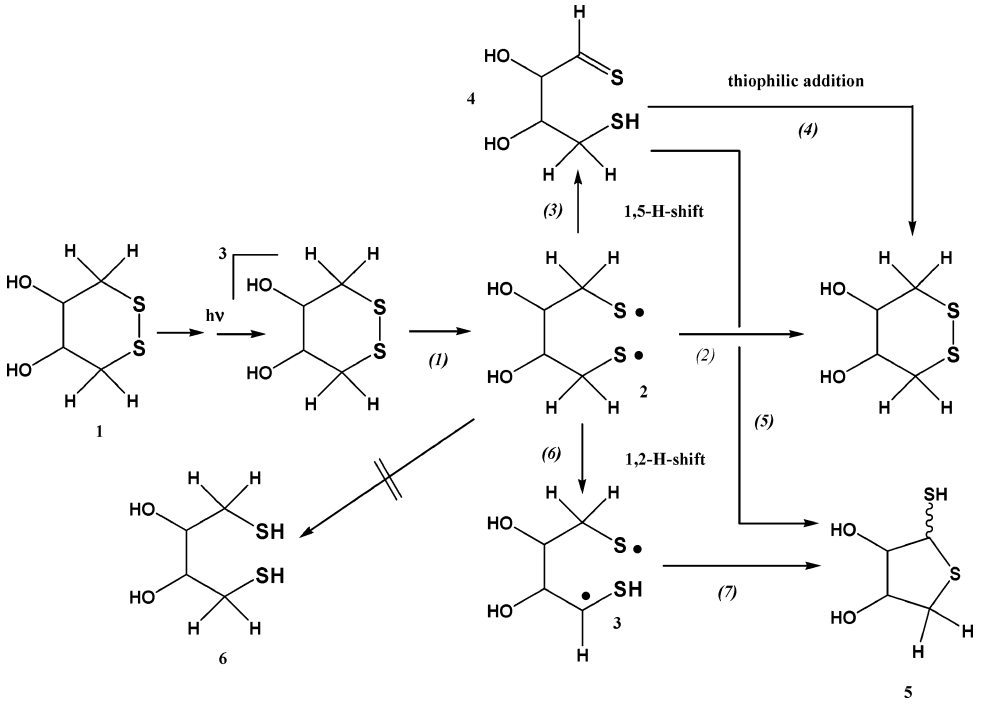

We recently established that the photolysis of DTT_{ox} in solution yields dithiyl radicals **2**, which ultimately form two isomers of 2,3-dihydroxy-1-mercaptotetrahydrothiophene **5** via either reactions 3 and 5 or reactions 6 and 7 (see Scheme 1).[9]

In methylene chloride (CH_2Cl_2), the dithiyl radical **2** abstracts a H atom from a second molecule of DTT_{ox}, demonstrating its suitability to initiate H-transfer reactions.[9] On the basis of the molecular similarity of **1** and **6**, we expected good cocrystallization of both compounds to permit chemical reactions in the solid state. We will show that dithiyl radical **2** indeed abstracts a H atom from **6** in the solid state, resulting in the formation of a thiyl radical. The latter will ultimately form 2,3-dihydroxy-1-mercaptotetrahydrothiophene through a reaction with molecular oxygen.

Experimental Section

Materials. D/L-DTT_{ox} and DL-1,4-dimercapto-2,3-butanediol (D/L-DTT) were obtained from Sigma-Aldrich Chemical Co. (St. Louis, MO) and used as received. If not stated otherwise, all experiments were conducted with D/L mixtures of these compounds. Optically pure L-DTT_{ox} was prepared by oxidation of L-DTT and preparative high pressure liquid chromatography (HPLC) separation. Methylene chloride (CH_2Cl_2) and HPLC-grade acetonitrile (CH_3CN) were purchased from Fisher Scientific (Pittsburgh, PA) and used as received. Water was distilled by a Labconco purification system. D_2O was received from Cambridge Isotope Laboratories, Inc. (Andover, MA).

Photochemical Reactions. Photochemical reactions were carried out either in a Rayonet photoreactor (Southern New England Ultraviolet Co., Branford, CT) or in a custom-built photolysis system. The Rayonet photoreactor was equipped with up to eight RPR-3500 lamps, which emit light between 305 and 410 nm, overlapping with the low-energy part of the UV absorbance of DTT_{ox} (absorbance ca. 250−325 nm; $\lambda_{max} = 280$ nm). The custom-built photolysis system was composed of an arc lamp power supply (model 68806; Oriel Instruments, Stratford, CT), a convective lamp housing (Oriel Instruments) equipped with a 100-W (ozone-free) xenon lamp, a monochromator (model 77250; Oriel Instruments), and an integrating sphere (Labsphere, Inc., North Sutton, NH). The light beam was guided into the monochromator with a fused-silica plano-convex lense (Oriel Instruments) and from the monochromator into the integrating sphere via a biconvex fused-silica lense (Oriel Instruments). From the integrating sphere, the reflected light was collected and quantified by a Labsphere integrating sphere system control (SC-5500; Labsphere, Inc.). Data acquisition was performed over an RS232 interface using software written in Delphi (Borland, Scotts Valley, CA). The photolysis sample was placed into the integrating sphere, and the monochromator wavelength was set to 297 ± 2 nm (slit width = 280 μm).

Sample Preparation. For photochemical experiments in the Rayonet photoreactor, either neat DTT_{ox} or physical mixtures of DTT_{ox} and DTT at different mass ratios were dissolved in 1 mL of methylene chloride in quartz test tubes. The methylene chloride was then evaporated using a vacuum pump (Barnant Co., Barrington, IL), leaving thin layers deposited on the walls of the quartz test tubes. After irradiation, the deposits were dissolved in 1 mL of acetonitrile and diluted to 1:20 (v/v) with purified water for analysis by reverse phase-HPLC (RP-HPLC). For studies of kinetic isotope effects, a physical mixture of DTT/DTT_{ox} (10:1; w/w) was dissolved in deuterium oxide. The samples were allowed to exchange for 4 h at 5 °C before lyophilization. Thin-layer deposits were then prepared as stated above.

For photochemical experiments in the integrating-sphere system, thin layers of sample were deposited on quartz windows (Hellma, Plainview, NY). A 5 mg/mL solution of DTT_{ox} and a 50 mg/mL solution of DTT were made in methylene chloride. Then, 100-μL aliquots of the individual solutions or a 1:1 (v/v) mixture of both solutions was placed on the quartz window, and the solvent was evaporated. Each window was placed individually into the integrating sphere and irradiated with 297-nm light for either 1−2 (DTT/DTT_{ox} mixtures) or 5 (DTT_{ox}) days. After irradiation, the deposits were dissolved in 1 mL of acetonitrile and diluted to 1:20 (v/v) with purified water for analysis by RP-HPLC.

HPLC Analysis. Product separation was carried out on a Hewlett-Packard 1050 instrument equipped with a UV detector. A 100-μL aliquot of diluted sample was injected using an Agilent Technologies 1100 autosampler onto a HPLC column (Phenomenex ODS, 250 × 4.5 mm) and eluted using a linear acetonitrile/trifluoroacetic acid gradient with UV detection at 214 nm. The mobile phase started with 5% mobile phase B [0.1% (v/v) trifluoroacetic acid/90:10 (v/v) acetonitrile/water] at 0 min and increased linearly to 30% mobile phase B within 30 min at a flow rate of 0.8 mL/min. Products were isolated and lyophilized for characterization.

Quantification of H_2O_2. Hydrogen peroxide (H_2O_2) was measured spectrophotometrically by detecting its titanium sulfate complex at 410 nm, using $\epsilon_{410} = 700$ L mol $^{-1}$ cm^{-1}.[10] To determine the limit of detection, a H_2O_2 standard curve ranging from 0 to 500 μM concentrations was prepared. We obtained a limit of detection of 10 μM. The standard curve was linear between 10 and 500 μM H_2O_2. Sample preparation and irradiation was as described above for photochemical reactions in the Rayonet photoreactor. After irradiation, samples were reconstituted with 1 mL of peroxide analyte solution [1% Ti-(IV), 10% H_2SO_4] and immediately analyzed by UV spectroscopy.

Solid-State NMR Spectroscopy. Solid-state NMR was used to determine the crystallinity of the solid deposits. As a result of the large mass quantity needed for analysis, deposits were prepared using a rotary evaporator instead of test tubes. Differing ratios of DTT/DTT_{ox} (10:1, 4:1, 2:1, and 1:1) were tested with a final mass of 1 g/deposit. Reagents were dissolved in 500 mL of CH_2Cl_2, and the solvent was removed using a rotary evaporator.

All ^{13}C spectra were acquired on a Chemagnetics CMX-300 spectrometer (7.05 T) using cross polarization (CP) and magic-angle spinning (MAS). Samples were packed into 7.5-mm zirconia rotors and spun at 4 kHz in a Chemagnetics probe outfitted with a Pencil spinning module. Samples were packed in the rotors under normal atmospheric conditions and Kel-F endcaps were used to hold the sample in the rotor. The variable-amplitude CP experiment was used along with the total suppression of spinning sideband pulse sequence and two-pulse phase-modulated decoupling. A 120-s pulse delay and a ^{1}H 90° pulse width of 4−4.5 μs was used. A contact time of 5.0 ms was also used for the maximum transfer of magnetization from the ^{1}H to the ^{13}C nuclei. The free-induction decay contained 1024 data points acquired at a dwell of 33.3 μs. To obtain a relatively high signal-to-noise ratio, 1024−2560 transients were acquired depending upon the component ratio. Spectra were externally referenced to tetramethylsilane using the methyl peak of hexamethyl benzene at 17.35 ppm.

X-ray Diffraction. X-ray diffraction patterns were obtained on a Bruker D8 Advance diffractometer equipped with a theta−theta goniometer. Cu Kα radiation was used to generate the diffraction patterns ($\lambda = 1.54$ Å) with an X-ray generator with the power setting at 40 kV and 40 mA. A step scan of 0.04° 2θ with 12 s/step from 15° to 40° 2θ was used. The samples for analysis were mounted on plastic sample holders, and to avoid any type of water adsorption during the course of the acquisition of the diffraction pattern, a thin polymer film was used to seal the sample in the holder.

Quantification of Residual Moisture. Solid deposits containing different ratios of DTT and DTT_{ox} were tested for residual moisture after dissolution in 0.5 mL of anhydrous methylene chloride (CH_2Cl_2). The total volume was injected into a Karl Fischer coulometer (Mettler Toledo, Columbus, OH) for titration analysis according to published procedures in the Annual Book of ASTM Standards (ASTM 1533-88). Samples were corrected for moisture in the solvent by titration of neat CH_2Cl_2.

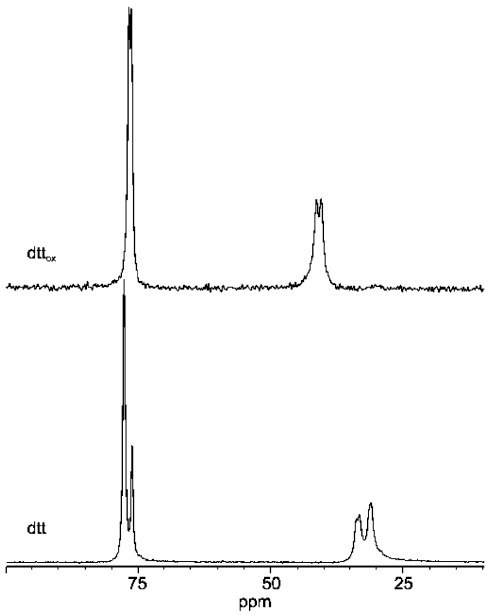

Figure 1. ^{13}C CPMAS NMR spectra of D/L-DTT_{ox} and D/L-DTT.

Results

Characterization of the Reaction Mixture. *Solid-State ^{13}C NMR.* NMR experiments were initially performed on the two native reactants DTT_{ox} (**1**) and DTT (**6**) to optimize the experimental parameters. Spectra of both compounds could be assigned using the same NMR acquisition parameters, making it easy to study mixtures of the two compounds. The spectra, shown in Figure 1, show that both compounds were crystalline and that mixtures of the two compounds would have resolved NMR spectra. In addition, a physical mixture containing a 10:1 (w/w) ratio of DTT/DTT_{ox} was also analyzed for comparison with the spectra of the solid deposits. Deposits were prepared using varying ratios (1:1, 2:1, 4:1, and 10:1, w/w) of DTT/DTT_{ox}. Figure 2 shows the spectra of these four deposits. The chemical shifts of the peaks in the spectra did not change. Changes are only observed in the relative intensity of the DTT_{ox} component as the ratio of DTT/DTT_{ox} changed. No additional peaks were observed. The presence of additional peaks would indicate possible interactions between the compounds as a result of additional bonding, either hydrogen or covalent bonding, because NMR spectroscopy is sensitive to changes in the local environment and short-range order.[11−13]

X-ray Diffraction. Diffraction patterns of DTT and DTT_{ox} indicated crystalline samples, as shown in Figure 3. The diffraction patterns for the solid deposits showed no changes in the observed peak positions, indicating that no change in the long-range order of the material had occurred (Figure 4A)[14] and that the sample was crystalline. The differences in the relative intensities observed for the reference compounds and the final deposit are possibly due to crystalline size and preferred orientation effects. In addition, the overall decrease in resolution of the samples containing DTT compared with that of the sample containing DTT_{ox} alone is due to the polymer film that was used to seal the DTT-containing samples to prevent moisture absorption by DTT. The use of a polymer film blocked both incident and refracted X-rays to and from the sample; therefore,

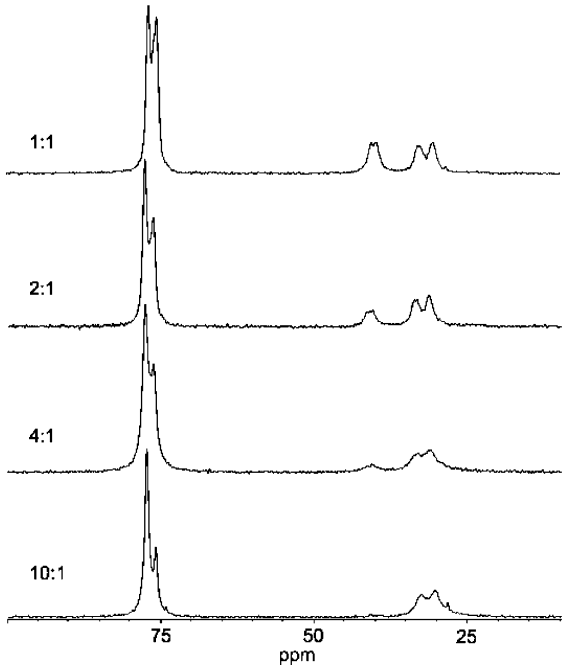

Figure 2. ^{13}C CPMAS NMR spectra of mixtures of D/L-DTT/D/L-DTT_{ox} at various ratios between 1:1 and 10:1 (w/w).

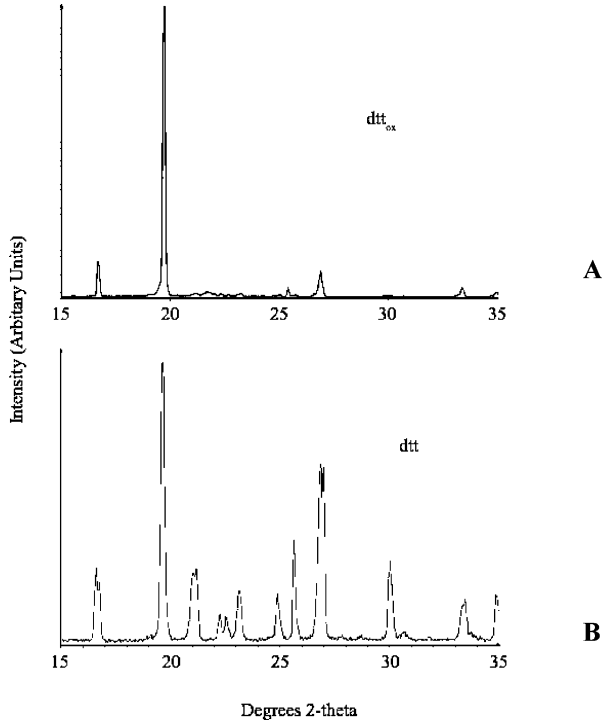

Figure 3. X-ray diffraction patterns of D/L-DTT_{ox} (A) and D/L-DTT (B).

the intensities observed for the DTT-containing samples were greatly diminished, lowering the quality of the diffraction pattern. A physical mixture of the two compounds yielded a similar diffraction pattern as the solid deposit (Figure 4B).

Product Characterization and Quantification. *Photolysis of DTT_{ox}.* The photolysis of solid D/L-DTT_{ox} resulted in the formation of two distinct products, labeled I and II in the chromatogram displayed in Figure 5. ^1H NMR and mass spectrometric analysis confirmed that products I and II represent two isomers of 2,3-dihydroxy-1-mercaptotetrahydrothiophene, **5**, that are identical to the products obtained during the photolysis of DTT_{ox} in either H_2O or CH_2Cl_2.[9] The yields of

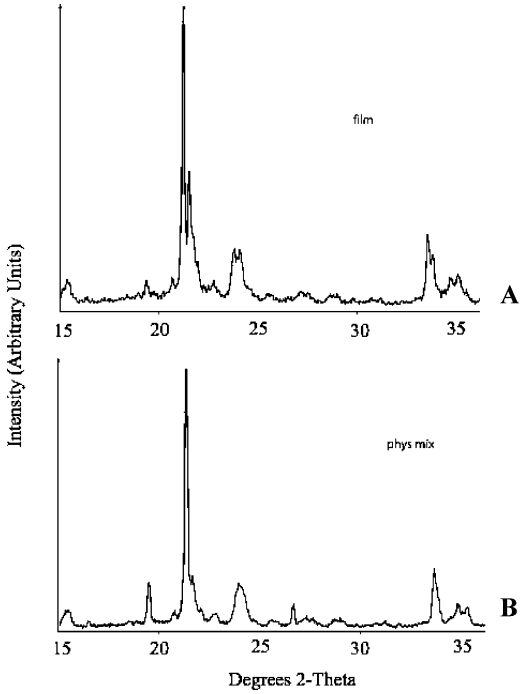

Figure 4. X-ray diffraction patterns of a solid deposit (A) or a physical mixture (B) of a 10:1 ratio of D/L-DTT/D/L-DTT_{ox}.

both product I and product II depended on the irradiation time, as shown in Figure 6. However, this dependence was not entirely linear. Products I and II represent the only products observed immediately after photolysis. However, upon prolonged storage (>12 h), these products degrade into secondary products, which have not been further characterized.

Photolysis of DTT/DTT_{ox} Mixtures. Solid deposits of mixtures containing various ratios of DTT/DTT_{ox} were prepared. The photolysis of these mixtures resulted in an increased yield of product I, depending on the weight fraction of DTT, and a generally decreased yield of product II, displayed in Figure 7. At a weight ratio of DTT/DTT_{ox} = 10:1, the photolytic yield of product I increased about 4-fold as compared with the yield of product I obtained with DTT_{ox} alone (i.e., in the absence of DTT), whereas the presence of DTT actually diminished the photolytic yields of product II. In control experiments, we verified that the photolysis of DTT alone did not result in any formation of products I and II (in these experiments, care must be taken to avoid any oxidation of DTT to DTT_{ox} during sample preparation). The levels of residual moisture were independent of the relative content of DTT, quantified as 9 ± 1% residual moisture, representatively, for DTT/DTT_{ox} ratios of 1:1, 4:1, and 10:1. Hence, the enhanced yields of product I and the lower yields of product II were not caused by different levels of residual moisture.

The absolute stereochemistry of products I and II was not determined as a result of the lack of an independent stereospecific synthesis. However, the data presented in Figure 8 show that especially the photolysis of optically pure L-DTT_{ox} produced significantly lower yields of product II compared with the photolysis of D/L-DTT_{ox}. For example, representatively, for a 10-min photolysis, the yields of product II were 88% lower during the photolysis of L-DTT_{ox} compared with that of D/L-DTT_{ox} and 50% lower for L-DTT/L-DTT_{ox} (10:1, w/w) compared with that of D/L-DTT/D/L-DTT_{ox} (10:1, w/w). These differences between the photolysis of L/D-DTT_{ox} and L-DTT_{ox} point to some conformational preference for product II formation

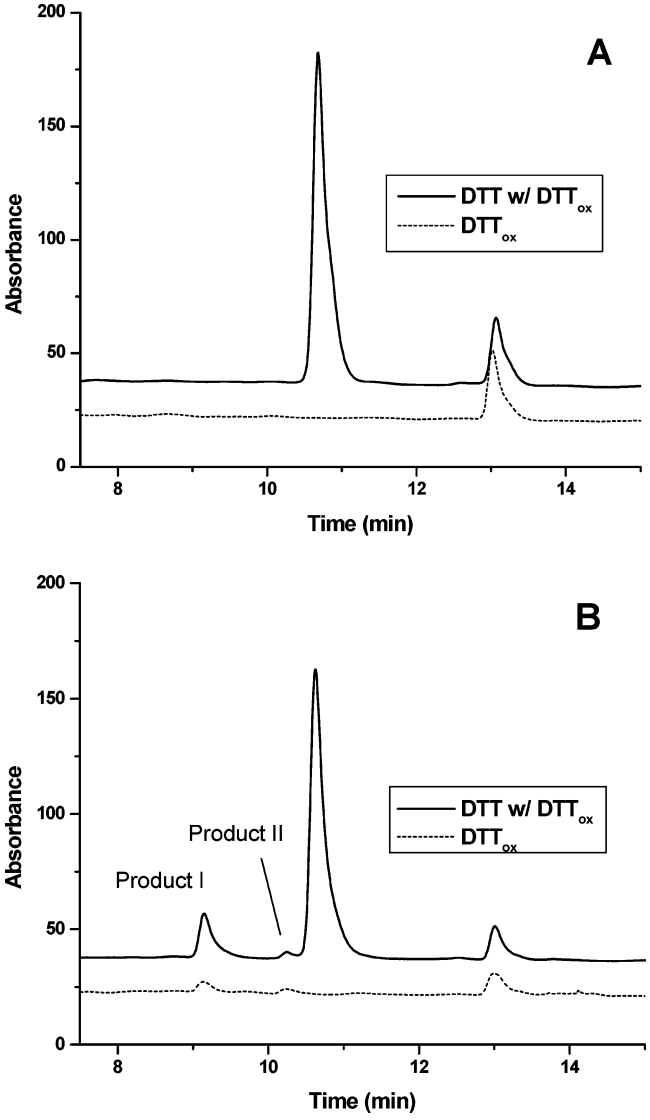

Figure 5. Product formation during the photolysis of DTT_{ox} in the presence or absence of DTT: (A) HPLC traces of control samples before photolysis; (B) HPLC traces of samples after 10 min of irradiation in the Rayonet photoreactor.

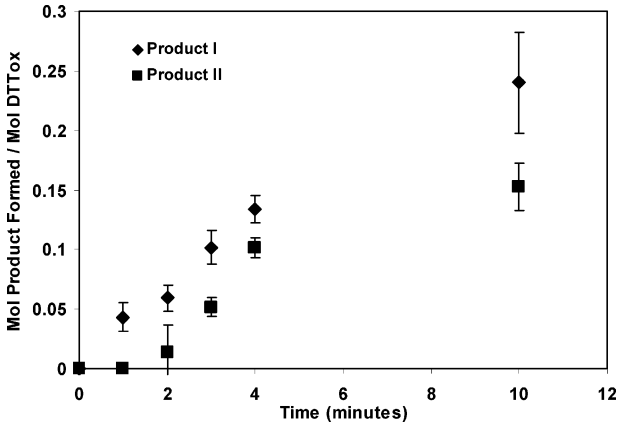

Figure 6. Yields of products I and II after specific amounts of time of photolysis in the Rayonet photoreactor. Yields are expressed as moles of product per moles of initial reactant, DTT_{ox}.

in the photolysis of the other epimer, D-DTT_{ox}. Importantly, such differences were not observed for product I formation.

Effect of Oxygen. The formation of products I and II was sensitive to the presence of O_2. Photolysis of DTT_{ox} under N_2

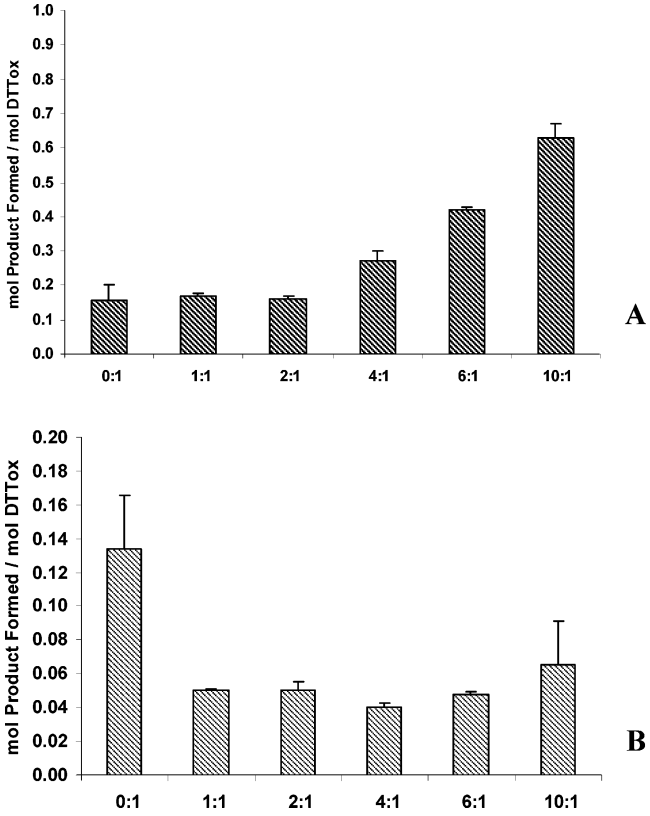

Figure 7. Effect of hydrogen-donor content (DTT) on the yields of (A) product I and (B) product II. Yields (after 10 min of photolysis) are expressed as moles of product per moles of initial reactant, DTT_{ox}.

(20-min purging of quartz vials with N_2) gave about 50% lower yields of products I and II compared with that of the photolysis of DTT_{ox} under air. The photolysis of 10:1 (w/w) mixtures of DTT/DTT_{ox} under N_2 gave about 27% lower yields of product I and 50% lower yields of product II compared with that of the photolysis under air. However, hydrogen peroxide was not detected after photolysis under air.

Isotope Effects. The large increase of product I in the presence of DTT suggests a photooxidation of DTT through a primary reactive intermediate from DTT_{ox}. A normal product isotope effect should be observable if this oxidation step contains a rate-determining hydrogen or proton transfer. To test for this, all the exchangeable protons of DTT and DTT_{ox} were exchanged in D_2O before lyophilization and the preparation of solid deposits of 10:1 (w/w) mixtures of DTT-d_4/DTT_{ox}-d_2 was conducted under an air atmosphere from which moisture was excluded through a $CaCl_2$-containing tube linking the quartz vial and the vacuum pump. Figure 9 shows that the photolysis of DTT/DTT_{ox} yields about 1.6-fold higher yields of product I and 1.8-fold higher yields of product II compared with that of the photolysis of DTT-d_4/DTT_{ox}-d_2.

Quantum Yields. In determining the quantum yields through eqs I and II, the integrating sphere was used, where P_{abs} is the amount of photons absorbed, P_c is the amount of photons reflected from a control sample lacking DTT_{ox}, and P_s is the amount of photons reflected from a sample containing DTT_{ox}.

$$\Phi_F = \text{moles of product/moles of absorbed photons} \quad \text{(I)}$$

$$P_{abs} = P_c - P_s \quad \text{(II)}$$

The moles of product produced were calculated from the peak areas of products I and II recorded during HPLC analysis (vide supra). The photolysis of D/L-DTT_{ox} alone gave quantum yields

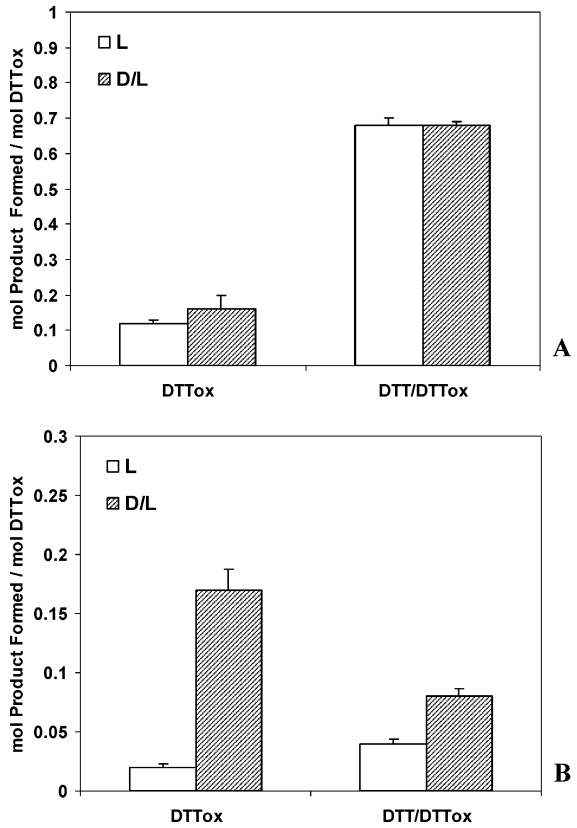

Figure 8. Quantitative comparison of product I (A) and product II (B) for the photolysis of D/L-DTT_{ox} and 1:10 (w/w) mixtures of D/L-DTT_{ox}/D/L-DTT with optically pure L-DTT_{ox} and L-DTT_{ox}/L-DTT. Yields (after 10 min of photolysis) are expressed as moles of product per moles of initial reactant, DTT_{ox}

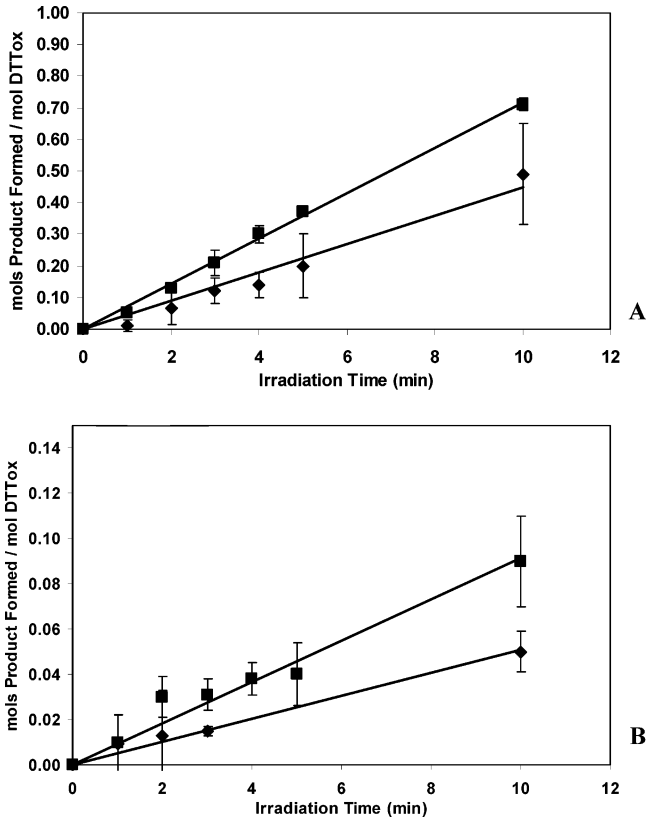

Figure 9. Product isotope effect on the production of products I (A) and II (B) from DTT-h_4 and DTT-d_4 at a 10:1 ratio of D/L-DTT/D/L-DTT_{ox}.

for the combined formation of products I and II of $\Phi_F = 0.39 \pm 0.02$, whereas the photolysis of 10:1 (w/w) mixtures of DTT/DTT_{ox} gave $\Phi_F = 0.87 \pm 0.13$.

Discussion

The following experimental features are important for a mechanistic discussion of the results. (i) The photolysis of thin deposits of crystalline DTT_{ox} under an air atmosphere yields two isomers of 2,3-dihydroxy-1-mercaptotetrahydrothiophene, **5**, products I and II, with a combined quantum yield of $\Phi_F = 0.39 \pm 0.02$. (ii) With the admixture of increasing amounts of DTT to DTT_{ox}, the yield of product I increases up to 4-fold, while the yield of product II decreases. The combined quantum yield of products I and II for 10:1 ratios of DTT/DTT_{ox} amounts to $\Phi_F = 0.87 \pm 0.13$, that is, is close to 1.0. (iii) Under a N_2 atmosphere, the yields of products I and II decrease by 27 and 50%, respectively. (iv) The formation of I and II shows normal product isotope effects of 1.6 and 1.8, respectively, when the exchangeable protons of DTT are replaced by deuterons.

The mechanism displayed in Scheme 2 (reactions 8−11) accounts for all the observations under air. These reactions have been formulated on the basis of known reactions of thiyl radicals in solution[15] or analogous processes of α-hydroxyalkyl radicals[16] (reaction 11). Dithiyl radical, **2**, abstracts a hydrogen atom from

SCHEME 2

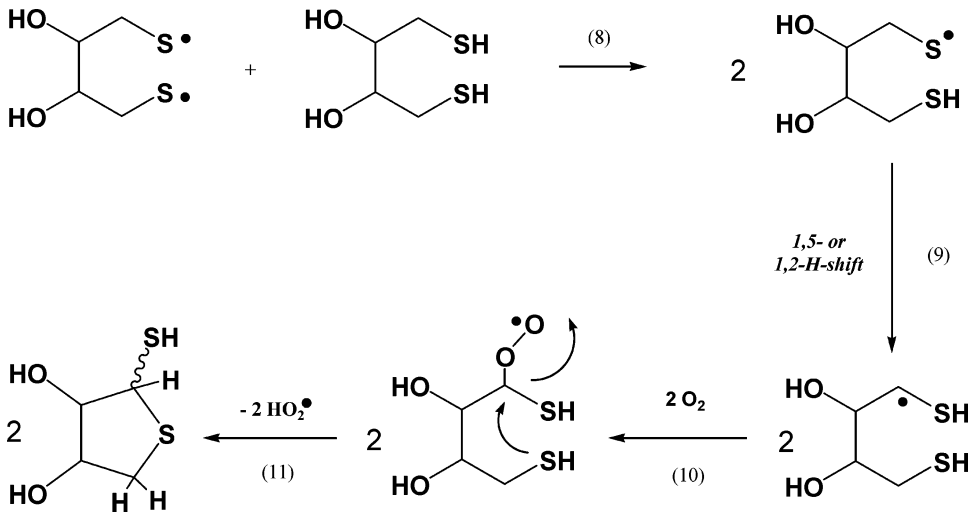

SCHEME 3

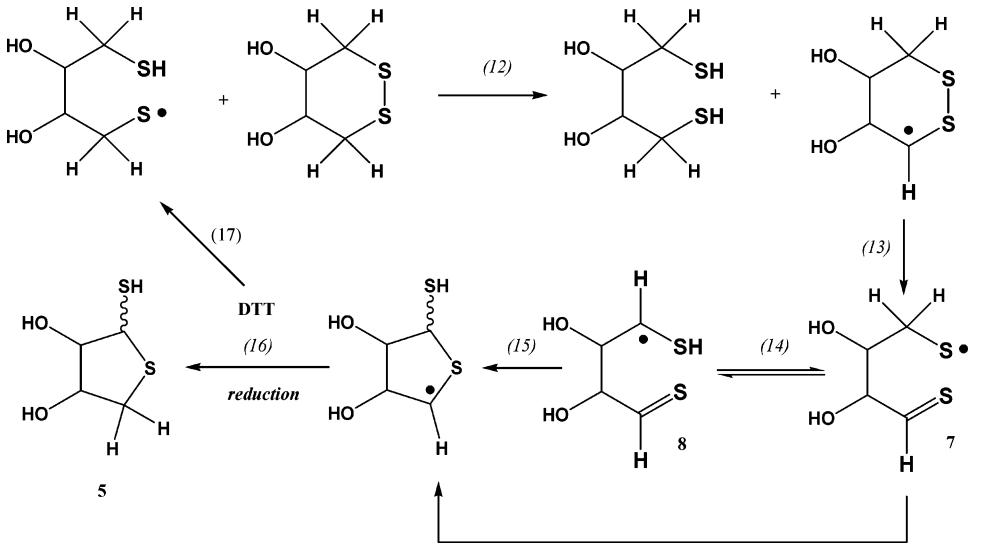

DTT to yield 2 equiv of monothiyl radicals (reaction 8). The latter either undergoes a 1,5-H shift or undergoes a 1,2-H shift (reaction 9) to yield α-mercaptoalkyl radicals, where the 1,5-H shift appears more probable on the basis of theoretical predictions[17] and the 1,2-H shift would likely be solvent-assisted.[18] These radicals add oxygen (reaction 10) and could eliminate a hydroperoxyl radical to yield **5** (reaction 11). One possible reaction, not shown in Scheme 2, is the reversible addition of oxygen to either the dithiyl or the monothiyl radical.[15] The reaction with the monothiyl radical would most likely yield DTT_{ox} and a hydroperoxyl radical,[19] that is, represent a pathway not leading to product **5**. Similarly, the addition of oxygen to the dithiyl radical **2** would not yield **5** but possibly a higher oxidation product of DTT such as α-disulfoxide or sulfonic acid;[20,21] product **5** is, however, the only reaction product observed immediately after photolysis.

In Scheme 2, reaction 8 is formulated as a formal H-atom transfer. In aqueous solution, such a H-atom transfer between thiyl radicals from *β*-mercaptoethanol and DTT occurs, in fact, quite rapidly with $k = 1.7 \times 10^7$ M^{-1} s^{-1}.[22] An alternative description of reaction 8 would be proton-coupled electron transfer.[23] The normal product isotope effect recorded for samples containing DTT-h_4 versus DTT-d_4 would be consistent with both mechanisms.

Reactions 8−11 clearly require molecular oxygen for product formation. An alternative mechanism, consistent with our photochemical results in solution,[9] which would operate independent of the presence of O_2, is displayed in Scheme 3. Also, this mechanism requires an initial reaction of dithiyl radical **2** with DTT to yield monothiyl radicals (reaction 8). Subsequently, the monothiyl radicals abstract H atoms from the methylene groups of DTT_{ox} (reaction 12), followed by C−S bond homolysis (reaction 13). The thiocarbonyl intermediate **7** may exist in equilibrium with intermediate **8**, and both intermediates serve as precursors for ring closure (reactions 14 and 15). Reduction by DTT would yield product **5**. Importantly, both mechanisms displayed in Schemes 2 and 3, respectively, have the potential to initiate chain oxidations: reaction 8 via formation of the known chain carrier for DTT oxidation, $HO_2^{\bullet}$ [19] and reactions 16 and 17 via formation of additional monothiyl radicals from DTT. However, at present, the quantum yields obtained for the photolysis of DTT/DTT_{ox} mixtures (10:1, w/w) only allow us to conclude that the addition of DTT increases the efficiency of product formation. Moreover, a variation of the light intensity had little effect on the photolytic yields of **5**, indicating that any potential chain reaction would only occur to a negligible extent.

The solid-state net-hydrogen-transfer reaction between diradical **2** and DTT presents an important contrast to earlier published work, where the reaction of a long-chain aliphatic-thiyl radical, $C_{18}H_{37}S^{\bullet}$, with a long-chain aliphatic thiol, $C_{18}H_{37}SH$, within thiourea clathrates proceeds via a net sulfur transfer to yield a perthiyl radical, $C_{18}H_{37}SS^{\bullet}$.[7] Hence, sulfur transfer is not a general phenomenon of a solid-state thiyl-radical reaction with a thiol. Instead, the extent to which either sulfur or hydrogen atoms are transferred will likely depend on the specific orientations of the reacting molecules toward each other in the solid state.

Conclusion

Our studies provide evidence for a H-atom transfer between thiyl radicals and thiols in crystalline solid deposits of DTT_{ox} and DTT. Though potential chain carriers are generated as a result of this process, no experimental evidence for a chain oxidation of the crystalline mercaptane was obtained.

Acknowledgment. This work was supported by a grant from Pfizer, Inc.

References and Notes

(1) Scheffer, J. R. In *Organic Solid State Chemistry*; Desiraju, G. R., Ed.; Elsevier: Amsterdam, 1987; pp 1−45.
(2) McBride, J. M. *Acc. Chem. Res.* **1983**, *16*, 304−312.
(3) Byrn, S. R.; Pfeiffer, R. R.; Stowell, J. G. *Solid-State Chemistry of Drugs*; SSCI, Inc.: West Lafayette, IN, 1999.
(4) Feng, X. W.; McBride, J. M. *J. Am. Chem. Soc.* **1990**, *112*, 6151−6152.
(5) Connors, K. A.; Amidon, G. L.; Stella, V. J. *Chemical Stability of Pharmaceuticals*; John Wiley & Sons: New York, 1986.
(6) Von Sonntag, C. In *Sulfur-Centered Reactive Intermediates in Chemistry and Biology*; Chatgilialoglu, C., Asmus, K.-D., Eds.; NATO ASI Series, Series A: Life Sciences; Plenum Press: New York, 1990; Vol. 197, 359−366.
(7) Faucitano, A.; Buttafava, A.; Mariani, M.; Chatgilialoglu, C. *ChemPhysChem* **2005**, *6*, 100−1107.
(8) Hadley, J. H., Jr.; Gordy, W. *Proc. Natl. Acad. Sci. U.S.A.* **1974**, *71*, 3106−3110.
(9) Barrón, L. B.; Waterman, K. C.; Filipiak, P.; Hug, G. L.; Nauser, T.; Schöneich, C. *J. Phys. Chem. A* **2004**, *108*, 2247−2255.
(10) Eisenberg, G. M. *Ind. Eng. Chem., Anal. Ed.* **1943**, *15*, 327−328.
(11) Tishmack, P. A.; Bugay, D. E.; Byrn, S. R. *J. Pharm. Sci.* **2003**, *92*, 441−474.

(12) Bugay, D. E. *Pharm. Res.* **1993**, *10*, 317−327

(13) Harris, R. K. *Nuclear Magnetic Resonance Spectroscopy*; John Wiley & Sons: New York, 1994; p 260.

(14) Guinier, A. *X-Ray Diffraction: In Crystals, Imperfect Crystals, and Amorphous Bodies*; Dover Publications: New York, 1994; p 254.

(15) Zhang, X.; Zhang, N.; Schuchmann, H.-P.; von Sonntag, C. *J. Phys. Chem.* **1994**, *98*, 6541−6547.

(16) Von Sonntag, C. *The Chemical Basis of Radiation Biology*; Taylor & Francis: London, 1987.

(17) Viskolcz, B.; Lendvay, G.; Körtvélysi, T.; Seres, L. *J. Am. Chem. Soc.* **1996**, *118*, 3006−3009.

(18) Konya, K. G.; Paul, T.; Lin, S.; Lusztyk, J.; Ingold, K. U. *J. Am. Chem. Soc.* **2000**, *122*, 7518−7527.

(19) Lal, M.; Rao, R.; Fang, X.; Schuchmann, H.-P.; von Sonntag, C. *J. Am. Chem. Soc.* **1997**, *119*, 5735−5739.

(20) Freeman, F.; Angeletakis, C. N. *J. Am. Chem. Soc.* **1981**, *103*, 6232−6235.

(21) Chatgilialoglu, C. In *The Chemistry of Sulphenic Acids and their Derivatives*; Patai, S., Ed.; John Wiley & Sons: New York, 1990; pp 549−569.

(22) Akhlaq, M. S.; von Sonntag, C. *Z. Naturforsch., C: J. Biosci.* **1987**, *42*, 134−140.

(23) Hammes-Schiffer, S. *Acc. Chem. Res.* **2001**, *34*, 273−281.